JOURNAL OF MATERIALS SCIENCE **34** (1999) 83–97

# Evaluation of the fatigue fracture resistance of unfilled and filled polytetrafluoroethylene materials

H. AGLAN, Y. GAN, M. EL-HADIK
*Mechanical Engineering Department, Tuskegee University, Tuskegee, AL 36088*
P. FAUGHNAN, C. BRYAN
*NASA Kennedy Space Center, Kennedy Space Center, FL*

Polytetrafluoroethylenes (PTFEs) and their composites are a special class of fluorocarbons with very high chemical resistance and wide service temperature. This makes them good candidate materials for load-bearing components exposed to harsh environments, including some space applications. In the present work, fatigue crack propagation (FCP) behavior of four materials from the fluorocarbon family, including PTFE without filler (virgin PTFE), PTFE with 15% glass fiber, PTFE with 15% graphite particles, and PTFE with 25% glass fiber, were studied. Tension/tension FCP experiments were carried out using single-edge notch (SEN) specimens under load control. The maximum stress was kept constant at 8 MPa for each material at a frequency of 3 Hz. The minimum to maximum stress ratio was 0.27. FCP data such as the number of cycles, crack length, and hysteresis loops were recorded in order to establish the crack speed, the energy release rate, $J^*$, and the change in work $\dot{W}_i$. Parameters that characterize the resistance of PTFEs to FCP have been successfully determined by the modified crack layer (MCL) model. These parameters are $\gamma'$, the specific energy of damage, which reflects the FCP resistance of the PTFE materials, and the dissipative characteristic of the materials, $\beta'$. It has been found that the MCL model describes the behavior of the PTFEs over the entire range of the energy release rate and discriminates the subtle effects introduced by changing the filler type and dosage as well as the processing conditions. The values of the specific energy of damage $\gamma'$ have been found to decrease by increasing the dosage of the fiberglass fillers. Graphite particulate filler also reduced the value of $\gamma'$ more than fiberglass filler for the same dosage. Microscopic analysis of the fracture surface in the stable crack propagation region of each material revealed that there exists a strong correlation between the value of $\gamma'$ and the amount of damage energy manifested by different mechanisms and species during the fatigue process. 

## 1. Introduction

Polymeric solids are being used in the manufacturing of an increasing number of load-bearing structural components such as gas transport systems, gears, hinges, springs, and mechanical arms. In part this has been driven by the trend toward lightweight engineering systems and the steady improvement in the mechanical properties of many polymers or plastics. Fluorocarbon polymers have proved to be a very good choice for use in motor seals, airplane gaskets, bearings, and O-rings [1–3]. PTFE is a self-lubricating fluorocarbon with an extremely low friction coefficient (below 0.1) that is used with or without fillers for diversified application purposes [4, 5]. PTFE has a working temperature range from −260 °C to 260 °C. It is chemically inert and does not absorb water, resulting in excellent dimensional stability. Its melting temperature is 327 °C, which is much higher than that of most other semicrystalline polymers. Blended with other plastics, metals, non-metallic fibrous materials (such as glass fiber) and fillers (such as graphite particles), PTFE-based composites are important materials for self-lubricating bearings and energy transmitting devices such as clutch plates. Graphite particles are also added in some applications to improve the poor thermal conductivity of PTFE. This improvement in conductivity is critical to the PTFE system since the mechanical properties of PTFE are highly temperature dependent. PTFE composites can also provide other desirable properties, such as toughness, resiliency, and oil resistance, that make them good candidate materials to meet NASA requirements for space applications [6].

To provide assurances that PTFE parts will withstand the rigors associated with their service life, more detailed characterizations of their deformation and fracture properties are demanded. Since many loads are cyclic in nature, the deformation and fracture response

to cyclic loads (fatigue) is of particular interest. Engineers and designers are well-aware of the insidious nature of structural damage resulting from repetitive loadings. Although one load excursion may not cause fracture, repeated stressing or straining to the same level (even less than the nominal yield strength or strain) will precipitate damage and eventual failure. Failure then occurs when some critical level of damage is accumulated to either fracture the component or render it incapable of satisfactorily performing its intended function. The actual service life of a PTFE product will then depend strongly on the number of stress or strain cycles experienced during its intended life span and the extent of damage accumulated per loading excursion.

As compared with metallic materials, the fatigue behavior of advanced polymeric systems has been studied less. Plumbridge [7] treated the fatigue of polymers and metals together; this attempt of generalization is useful in view of the need to bring together different kinds of specialists. Shortly thereafter, in a precursor to this article, the authors critically reviewed the field of fatigue in polymers, with emphasis on the role of molecular structure and composition, and micromechanisms [8]. Recently, Stachurski [9] reported the deformation mechanisms and strength in amorphous polymers. The essentials of continuum mechanics, phenomenology, and molecular theories of yield have been presented. Some recent computer modeling results that provide some fundamental aspects in failure initiations of polymers are also given. Historically, the earliest report on fatigue in polymers was published in 1950. Superposition principle and the fracture mechanics approach were used, and an outline of fatigue testing was presented by Dillon [10]. Following Dillon's work, Rosen [11] presented theoretical and phenomenological aspects of the kinetics, energitics, and morphology of polymer fracture. In particular, Worlock and Newman [12] and Landel and Fedors [13] discussed fracture surface topography and failure in amorphous polymers, respectively. Following an overview of fracture (including fatigue) in polymers [14], Andrews published a clear exposition of his view on static and fatigue failure [15]. In later reviews, Andrews also described the distinction between creep and thermal and mechanical aspects of fatigue (a distinction not always recognized) and outlined fracture mechanics approaches to the characterization of fatigue [16]. Some effects of composition were also discussed by Bucknell *et al*. [17]. An interesting discussion of fatigue is given in a chapter on fracture by Vincent [18] and in a review by Hearle [19] of fatigue in polymers, especially fibers. Later reviews by Beardmore and Rabinowitz [20] and by Schultz [21] emphasize the phenomenological aspects and micromechanism involved. General discussions of fracture in multicomponent systems are provided by Bucknell [22, 23]; Owen [24] and Harris [25] emphasize fatigue in fibrous composites. Critical reviews of the molecular aspects of fracture and of current fracture mechanics approaches are provided by Andrews and Reed [26] and Williams [27], respectively; these topics are also discussed in detail by Kausch [28].

One of the typical failure modes of polymers is formation and propagation of crazes, owing to strain-hardening of fibrils that span the craze [29, 30]. Most of the studies on crazing are based on monotonic load conditions such as tensile and creep test conditions. Since crazes can also form under small-scale yielding conditions [31], however, their formation and propagation are also very significant in the fatigue failure of polymers. Criteria for the fracture of polymeric materials have been investigated by Brown [32], who presented a stress intensity approach on craze failure. The craze is assumed to fail under different temperature and the load frequency or rate of deformation by scission of the first fibril directly ahead of the crack tip. The failure criterion is

$$\frac{K_{\text{tip}}}{(\pi d)^{1/2}} = \xi F, \tag{1}$$

where $K_{\text{tip}}$ is the local crack tip stress intensity factor, $d$ is the diameter of the fibril, $\xi$ is the number of entangled strands per nominal unit craze area, and $F$ is the force needed to break the backbone of a polymer chain.

Probabilistic models have been successfully applied to treat the failure of elastic materials such as metallic materials and fiber-reinforced composites with defects [33]. These models are based on some stringent assumptions, however. Limitations in the application of these models in polymer fatigue failure analysis still remain a big problem.

Energy consideration, in some cases, is more accurate than other approaches are to assess the failure behavior of polymers. Sue *et al.* [34] performed SEN three-point-bend fracture toughness measurements. The critical strain energy release rate ($G_{Ic}$) is obtained based on the relationship [35]

$$G_{Ic} = \frac{K_{Ic}^2(1 - v^2)}{E}, \tag{2}$$

where $E$ is the Young modulus and $v$ is Poisson's ratio, $K_{Ic}$ is the plane strain critical stress intensity factor. This model is based on brittle materials complying with linear elasticity, however, and is only applicable to cases of small-scale yielding or deformation, such as the failure of carbon and carbon composites [36]. For failure analysis of polymers with considerable non-linear deformation, limitations are obvious.

Fracture driving force or fracture energy may also be determined by tear test for elastomeric materials. The energy can be expressed as tear strength $G_c$, and the related model was proposed by Ahogon and Gent [37] as

$$G_c = 2 f \lambda^2 / t, \tag{3}$$

where $f$ is the force to propagate a tear, $t$ is the torn thickness, and $\lambda$ is the swelling ratio that is equal to unity for dry specimens. For cracked specimens, the tear energy can also be calculated from the following equation [38]:

$$G_c = 2\text{k}Wa, \tag{4}$$

where k is a material constant depending on the expansion rate, $W$ is the strain energy density, and $a$ is the crack length. It has been found [39] that for the first 20% of the specimen width, the value of the energy release rate ($J^*$) and the tearing energy $G_c$ agree reasonably well with each other when the model was applied for fluoroelastomers, whereas significant discrepancy exists for the rest of the specimen width, which means that there is limited applicability of the use of tearing energy to describe the failure behavior of elastomers. Wang and Chang [40, 41] proposed a cutting and pulling method based on the studies of styrene-butadiene-styrene block copolymers. The fracture energy $G_c$ is calculated from the sum of energies expended in both pulling and cutting:

$$G_c = P + C, \tag{5}$$

where $P$ is the pulling energy and $C$ is the cutting energy. The essential consideration of this approach is the same as tearing energy approach and thus undergoes the same limitations.

Hornsby and Premphet [42] investigated the fracture of polypropylene. A procedure to determine the $J$-integral value for crack initiation was provided. In their work, $J_c$ is defined as the crack initiation energy or the energy required to create new surfaces. To determine this parameter, a graphical approach, called "the blunting line concept" was adopted, using the following expression:

$$J = 2\sigma_y \Delta a, \tag{6}$$

where $\sigma_y$ is the yield stress and $\Delta$a the incremental growth in crack length. In this method, the crack tip is assumed to be blunted with a semicircular geometry prior to initiation. The crack initiation energy, $J_c$, is the value of $J$ at intersection of the crack blunting line and the resistance, $R$, curve. This technique is suitable for describing failure criteria in many ductile or impact-resistant polymers. It is very difficult to obtain $J_c$ in some cases, however, because crack blunting cannot be observed totally.

To predict long-term performance or durability of polymers, investigation of the slow crack mechanisms is necessary. Generally, fatigue tests on polymer specimens are applied. Fatigue crack propagation in specimens of different geometries can be related by a meticulously designed fatigue test [43, 44]. Generally, the kinetics of fatigue is described by a power law proposed by Harris and Erdogan [45] in the following equation:

$$da/dN = \mathrm{A}(\Delta K)^{\mathrm{n}}, \tag{7}$$

where $da/dN$ is the average crack speed, $\Delta K$ is the crack driving force, and A and n are fitting parameters that depend on both the material properties and the fatigue test conditions, including the test stress amplitude and frequency. A major limitation of the power law is that the constants A and n do not fit the experimental data over the entire range of the crack driving force as indicated by Aglan *et al.* [46] as well as by Sancaktar [47]. This reveals the difficulties encountered in developing a unified unit of measuring the entire range of crack propagation and failure. Thus, the power law equation cannot adequately describe fatigue crack propagation over the entire range of energy release rate for many kinds of materials, especially polymers such as PTFEs.

The present work deals with fatigue crack propagation analysis of PTFE and its composites. The MCL model is employed to extract the specific energy of damage characteristic of the composites' resistance to fatigue crack propagation. The MCL model requires the measurements of crack length and the hysteresis loop at a different number of cycles during fatigue testing. An outline of the MCL model will be presented in the next section. The current investigation deals with the fatigue behavior of different PTFE materials with different compositions and processing conditions. The MCL model can provide a basis on which the relationships between the structure or the processing conditions, or both, and the resistance of the materials to fatigue crack propagation can be established. This is critical because the mechanical and fracture properties of polymers are strongly dependent on the composition and processing conditions [48]. Such relationships can provide guidelines for the development of novel PTFE systems with superior resistance to fatigue cracking and aid in their lifetime assessment.

## 2. Modified crack layer model

The development of fatigue crack–resistant polymers such as PTFEs necessitates a thorough understanding of their viscoelastic behavior. Recently, the MCL model has been proposed [49]. The capability of this approach to discriminate the subtle effects introduced by different chemical structures and processing conditions in various materials has been demonstrated [50–55].

The MCL model is expressed as

$$T\dot{S} = (J^* - \gamma' a)\dot{a} + \dot{D}, \tag{8}$$

where $T$ is the "ambient" temperature and $\dot{S}$ is the rate of change of the entropy of the system comprising the crack and the surrounding damage; $\dot{D}$ is the rate of energy dissipation on material transformation associated with active zone evolution; $a$ is the crack length; $\dot{a}$ is the crack speed, which can be expressed as $da/dN$ for cyclic fatigue, $N$ being the number of cycles; and $\gamma'$ is the specific energy of damage characteristic of the material's resistance to fatigue crack propagation.

At minimum entropy, the term $T\dot{S} = 0$ and Equation 8 can be written as

$$\dot{a} = \frac{\dot{D}}{(\gamma' a - J^*)} \tag{9}$$

The energy release rate $J^*$ can be evaluated experimentally. For stress control fatigue where $P$ is the

potential energy (area above the unloading curve) at each crack length $a$, and $B$ is the specimen thickness,

$$J^* = \frac{1}{B}\left(\frac{\partial P}{\partial a}\right) \tag{10}$$

Under strain control fatigue, $J$ can be used instead of $J^*$, and it is expressed as

$$J = -\frac{1}{B}\left(\frac{\partial U}{\partial a}\right), \tag{11}$$

where $U$ is the strain energy (area under the loading curve at the corresponding crack length $a$).

It has been shown [49, 50] that the cyclic rate of energy dissipation $\dot{D}$, associated with stress control loading can be expressed as

$$\dot{D} = \beta' \frac{dW_i}{dN} = \beta' \dot{W}_i \tag{12}$$

where $\beta'$ is the coefficient of energy dissipation. The quantity $\dot{W}_i$ is the change in work expended on damage formation and history dependent viscous dissipative processes within the active zone of the propagating crack. It was also shown [50] that

$$\dot{W}_i = \frac{1}{B}(H_i - H_o), \tag{13}$$

where $H_i$ is the area of hysteresis loop at any crack length and $H_o$ is the area of the hysteresis loop before crack initiation.

Substituting Equation 12 into Equation 9 and rearranging gives

$$\left(\frac{J^*}{a}\right) = \gamma' - \beta'\left(\frac{\dot{W}_i}{\left(\frac{da}{dN}\right)a}\right) \tag{14}$$

The quantities $J^*$, $da/dN$, $\dot{W}_i$, and $a$ can be measured during fatigue crack propagation experiments as previously reported [49–55]. It was also shown that if the quantities between brackets in Equation 14 are plotted in the $x$–$y$ domain, a straight line is obtained that attests to the fact that the theory is in accord with experimental results. This will directly give the value of the specific energy of damage $\gamma'$, which is the intercept of the straight line. The value of $\beta'$ is the slope of the straight line.

It should be emphasized that the $\gamma'$ criterion is based on the measurement of more fundamental parameters related to the fracture behavior of materials than any other fatigue law. These are the change in work $\dot{W}_i$ expended on damage formation and history dependent viscous dissipation processes, the volumetric amount of damage that is taken as a linear function of the crack length, the conventional crack speed, and the energy release rate $J^*$. Equation 14 will be employed in the current work to evaluate the fatigue fracture resistance of four PTFE materials with various reinforcement or filler and processing conditions.

## 3. Materials and experimental

Four materials from the PTFE family were used in the present study. These are

Virgin PTFE
15% glass fiber–reinforced PTFE
15% graphite-filled PTFE
25% glass fiber–reinforced PTFE

Specimens for the fatigue testing were cut to the dimensions 178 mm in length by 22 mm in width. A straight notch was made with a very sharp razor blade at the center of one free edge of the specimens. The notch depth was 2 mm. The gauge length of the specimens was 100 mm. These samples were tested using an MTS 810 hydraulic testing machine equipped with a 4450 N load cell. Tension-tension fatigue tests were conducted at room temperature under load control conditions using a frequency of 3 Hz. The maximum tensile stress applied to all materials was 8 MPa with a minimum to maximum stress ratio of 27%. The crack length at various intervals of number of cycles was recorded during the test. A traveling optical microscope was used to view the crack tip region to measure the crack length and capture the damage associated with the crack advance. Typical samples were used for both the fatigue propagation analyses and the fracture surface examinations. In order to compare the results among different materials, the testing conditions were kept the same. The stress was calculated based on the original cross-sectional area before testing.

The fracture surfaces and associated damage zones were cut away from fatigue-failed specimens for the four PTFE materials and sputter coated with gold–palladium alloy using an Hummer 6.2 coating system. The fracture surfaces were examined using a Hitachi S-2150 scanning electron microscope. The micrographs were recorded on Polaroid 55 film.

## 4. Results and discussion

In the following section, experimental FCP data will be used to obtain the crack propagation rate $da/dN$, the energy release rate $J^*$, and the change in work $\dot{W}_i$. The specific energy of damage, $\gamma'$, a material parameter characteristic of the resistance to FCP, can be then extracted from the MCL model using Equation 14. The analyses necessary to evaluate these parameters are presented next. It should be mentioned that the data reported here are an average of three fatigue specimens and that the scatter in the data was about 10%. Detailed experimental results and the related analysis will be given in the five parts as below.

### 4.1. Fatigue crack propagation rate

As described in the experimental section, the crack length was measured from the edges of the notched crack using a traveling optical microscope, at various intervals of number of fatigue cycles. A plot of the crack propagation length, $a$, versus the number of cycles, $N$, for the four precracked PTFE materials under consideration is shown in Fig. 1. The slope of the curves in

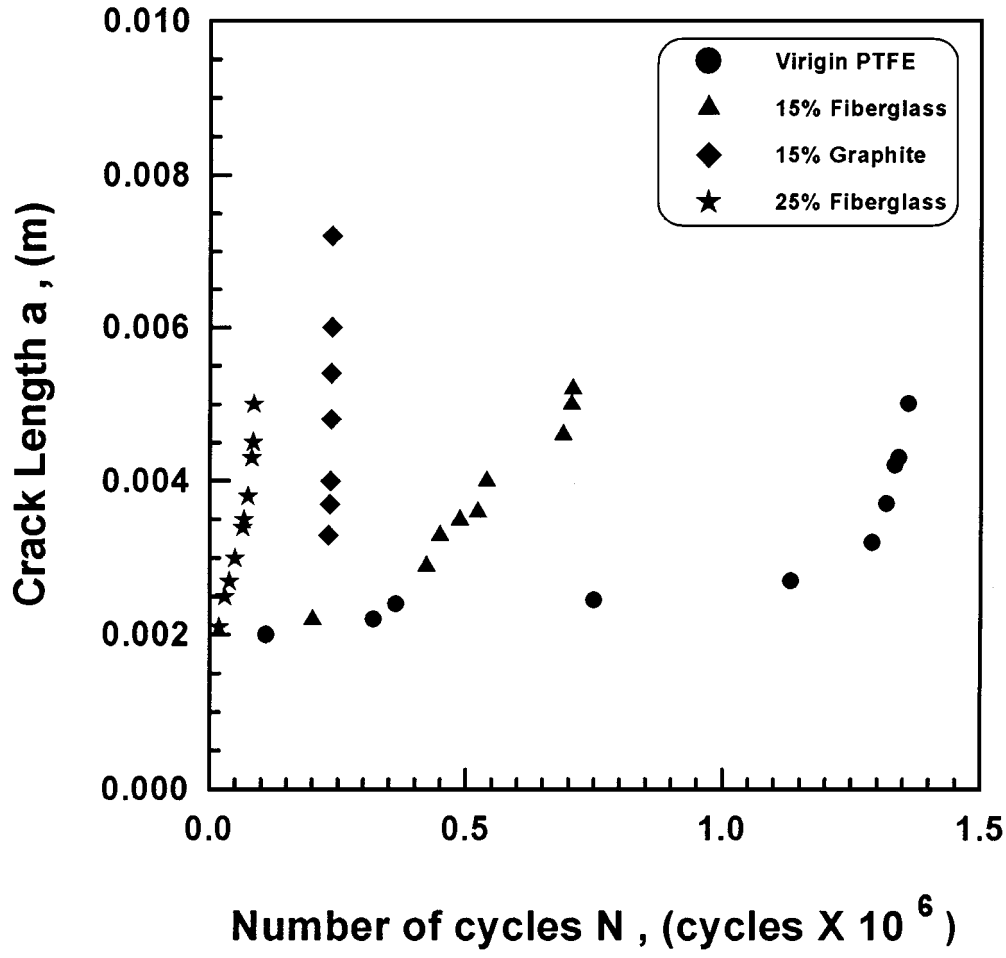


*Figure 1* Fatigue crack length versus the number of cycles for four PTFE materials.

Fig. 1 is taken as the average crack speed at each crack length. Both the initiation and propagation lifetimes are the highest for the virgin PTFE compared with the other three PTFE composites at the same stress level. The total lifetime of the virgin PTFE is nearly 1.5 million cycles. The figure also indicates that for the PTFE composite containing 25% fiberglass, cracking began at about 17,000 cycles and advanced steadily, reaching its fatigue life at about 85,000 cycles. Cracking started at about 20,000 cycles in both the 15% graphite PTFE composite and 15% fiberglass PTFE composite. The 15% graphite PTFE composite cracked more rapidly than did the specimens containing the same content of fiberglass. The 15% graphite PTFE has a total fatigue life of about 235,000 cycles. The PTFE composite specimens containing 15% fiberglass reached the fatigue life of more than 700,000 cycles, which is about three times that of 15% graphite PTFE. The slope of the curves in Fig. 1, at each crack length or at the corresponding number of cycles, will be calculated to obtain the FCP rate.

The crack propagation speed can be ranked, from fast to slow, as 25% fiberglass PTFE > 15% graphite PTFE > 15% fiberglass PTFE > virgin PTFE. From this result, it seems that the inclusion of fillers in the composite materials increased the fatigue damage sensitivity. Generally, adding fillers into the PTFE materials can enhance thier compressive static load-bearing ability and improve their thermal stability and creep resistance. The hardness of a PTFE can be also increased by the addition of filler. In some cases, special physical properties such as electrical conductivity and thermal conductivity can also be improved by introducing fillers into the PTFEs. In addition, cost reduction is also a consideration for filler addition. For the PTFE composites containing fiberglass filler, the higher the content of fiberglass, the less the FCP resistance, correspondingly, the shorter the fatigue life. It is also obvious that the shape of the filler is another factor that determines

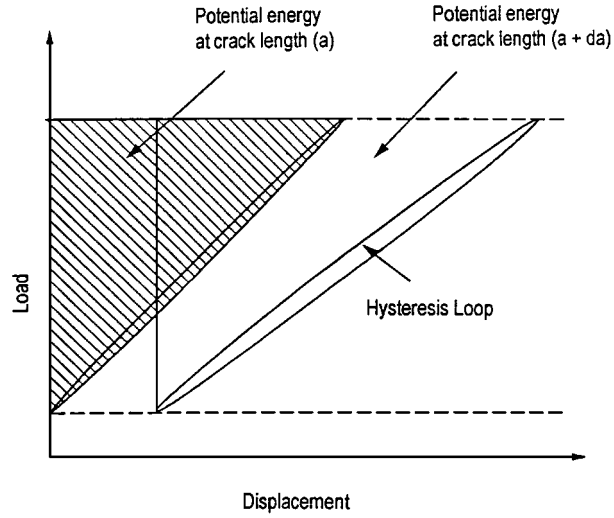


*Figure 2* Schematic representation of the potential energy measurements from the hysteresis loops for stress-controlled fatigue of the PTFE composites.

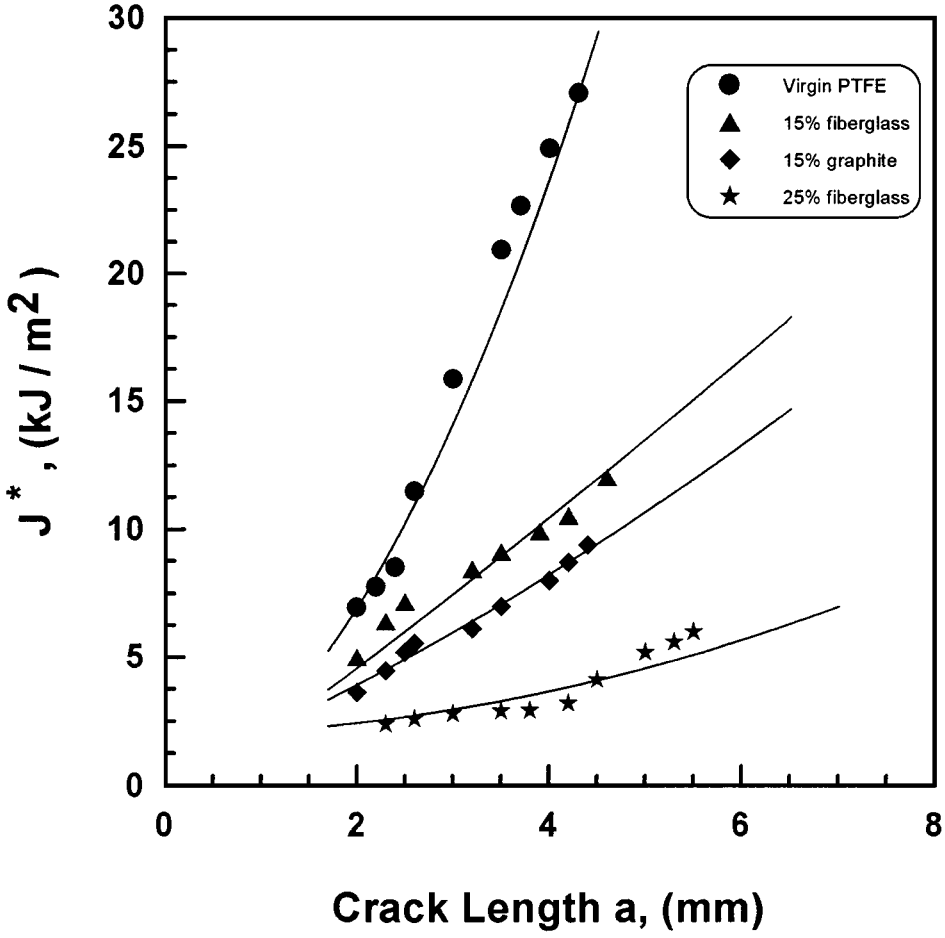


*Figure 3* Energy release rate, $J^*$, versus the fatigue crack length for four PTFE materials.

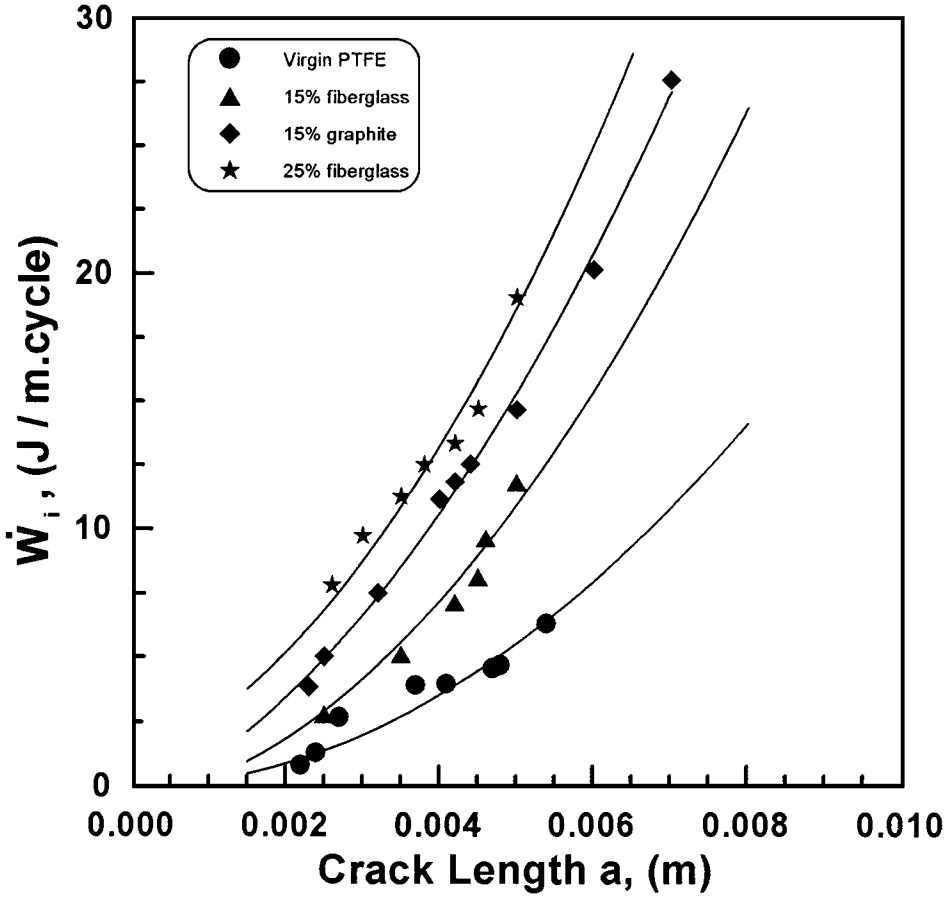


*Figure 4* Changes in work, $\dot{W}_i$, versus the fatigue crack length for the PTFE materials.

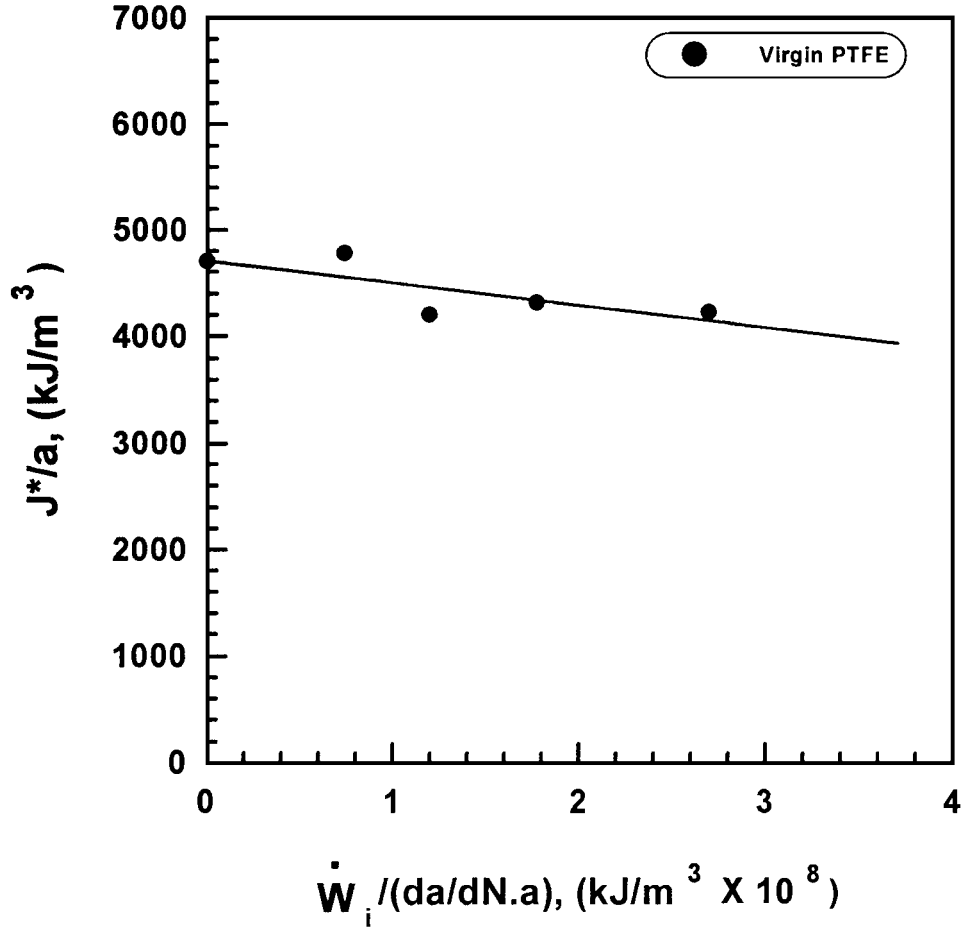


(a)

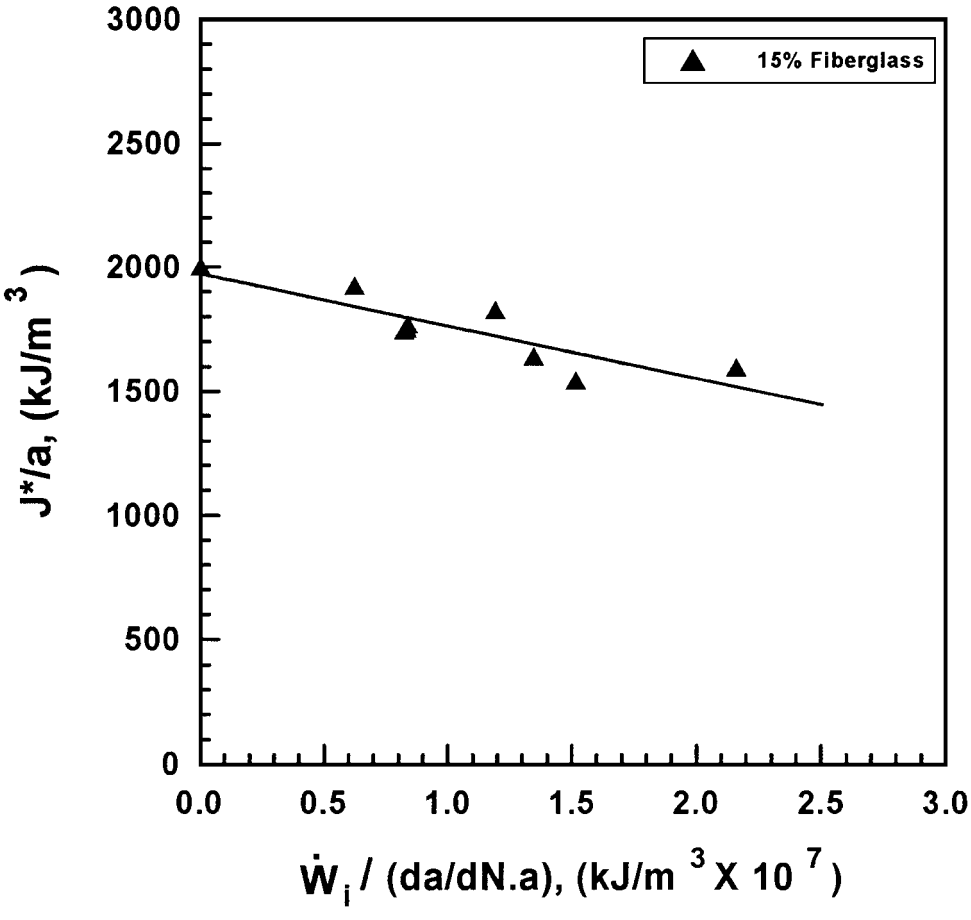


(b)

*Figure 5* FCP data for the specimens to obtain $\gamma'$, using the MCL model. (a) virgin PTFE, (b) 15% fiberglass PTFE, (c) 15% graphite PTFE and 25% fiberglass PTFE. *(Continued)*

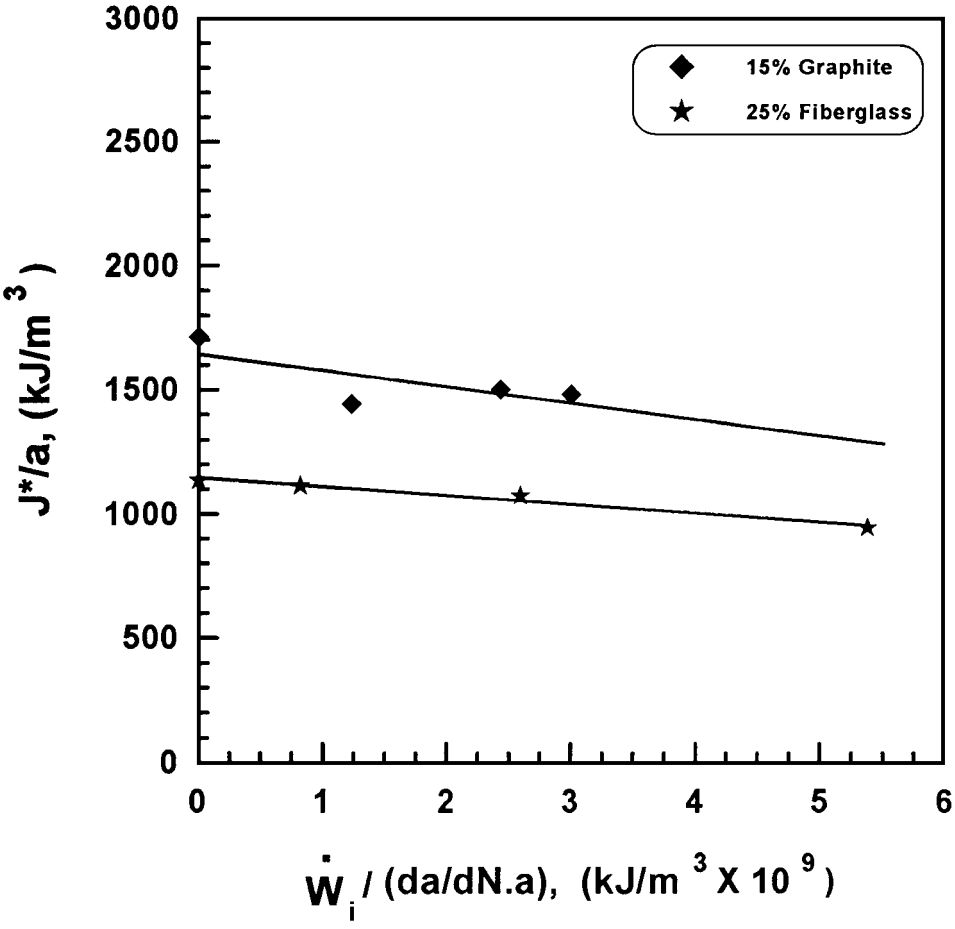


(c)

*Figure 5 (Continued).*

the FCP behavior of the PTFE composite materials. Particulate filler in comparison with fiber filler, at the same dosage, tends to embrittle the material.

## 4.2. Energy release rate

The potential energy, $P$, was calculated from the hysteresis loops recorded at intervals of number of cycles as the area above the unloading curve. This is shown schematically in Fig. 2. On this basis, the relationship between the potential energy and the FCP length, $a$, was established. The energy release rate, $J^*$, was evaluated at increments of crack length from the area above the unloading curve (potential energy: $P$) of the hysteresis loops of each PTFE composite. Since the fatigue tests are performed under stress control, $J^*$ can be calculated from the slope of the relationship between the potential energy and the crack length as described by Equation 10. In the ongoing analysis, the values of $J^*$ were measured experimentally from the actual tests on the five PTFE materials. This would make it more representative of the fatigue failure behavior of the chosen PTFE materials than the calculated elastic energy release rate or tearing energy. Fig. 3 illustrates the average value of energy release rate $J^*$ as a function of the crack length for the various PTFE materials. This is based on three identical specimens for each material. At a given value of crack length, the average value of $J^*$ for the virgin PTFE material is much higher than that of the other three kinds of PTFE materials. The $J^*$ of the 25% fiberglass-filled PTFE is the lowest of the four materials tested. Furthermore, the $J^*$ decreases with the increasing filler content in the materials. Again, the values of $J^*$ at different crack lengths will be used for the MCL model validation and $\gamma'$ determination.

For virgin PTFE, it has the close packing of the fluorine pendant groups, which provides a high molecular cohesion for the polymer chains [56]. When fillers such as fiberglass and graphite were introduced, the molecular chains of the PTFE partially separated from those sites where fillers exist. To some extent, the close packing state of the filled material is interrupted, resulting in a remarkable reduction in the fracture toughness. The greater the filler content, the more "brittle" the material. It can be observed from Fig. 3 that the higher the content of fiberglass filler in the PTFE composite, the lower the value of $J^*$ at the same crack length.

Particulate-shaped filler changes the $J^*$ of the materials more than fibrous filler does. In Fig. 3, the 15% graphite particle PTFE shows smaller values of $J^*$ than does the 15% fiberglass PTFE. Since fiber fillers or reinforcement in the composite materials tend to bridge the matrix, whereas particles cannot, crack propagation became easier under the same level of stress intensity in the particle-filled materials.

The results shown in Figs 1 and 3 are in good agreement with each other. Higher values of $J^*$ correspond to a longer lifetime and slower FCP speed. The above analysis will be used in the MCL model to evaluate the fatigue resistance of these PTFE materials.

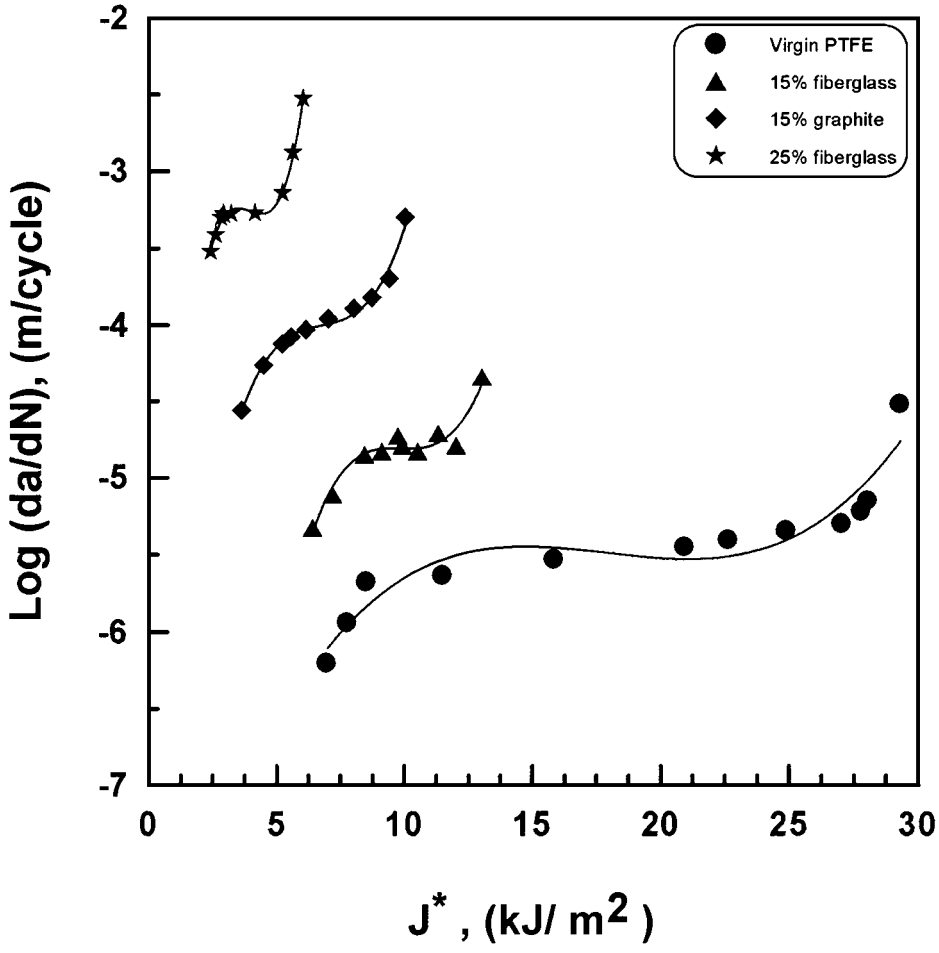


*Figure 6* The FCP speed versus the energy release rate for the four PTFE materials.

### 4.3. The change in work

The quantity $\dot{W}_i$, which is the "change in work," is calculated from the change in area of hysteresis loops recorded during the fatigue experiments. In this study, the hysteresis area was measured using a planimeter as the area within the respective hysteresis loops. The hysteresis energy $H_i$ is then used for the determination of change in work. In viscoelastic materials, $\dot{W}_i$ includes work expended on damage processes associated with crack growth and history-dependent viscous dissipation processes [49]. Both processes are irreversible. In practice, the $\dot{W}_i$ value is measured directly as the area of the hysteresis loop at any crack length ($a$) minus the area of the loop just before crack initiation, divided by the thickness of the specimens as given by Equation 13. The change in work $\dot{W}_i$, versus the crack length for each PTFE composite material is shown in Fig. 4.

The four materials exhibit the same trend in $\dot{W}_i$ over the entire range of crack lengths. As the crack increases, $\dot{W}_i$ increases. This indicates that the damage species for each of these four materials remain the same, and their elastic-plastic behavior is similar over the entire range of the crack length. The value of $\dot{W}_i$ for the 25% fiberglass PTFE, however, is the highest for the same crack length, whereas that of the virgin PTFE is the lowest.

Since the fatigue tests were performed under stress control, the smaller the $\dot{W}_i$, the greater the elastic behavior of the material should be. The molecular chain of the material retains more integrity during the fatigue damage process. It may be concluded that the virgin PTFE has less of a tendency to be damaged in service or under cyclic loading than the 25% fiberglass does. Introducing graphite particles to the PTFE matrix in the same dosage as that of fiber filler leads to a greater increase in irreversibility in deformation. This indicates that the deformation reversibility of the PTFE has been changed by fillers with different shapes and that the aspect ratio of the filler also contributes to the deformation irreversibility to some extent. It also seems to be true that the PTFE with graphite particles becomes more sensitive to damage under cyclic load than do PTFE composites with fibrous fillers because of the higher tendency of the particles to debond from the PTFE matrix. Indeed it is much easier for graphite particles to debond from the PTFE matrix than fibrous reinforcement, such as fiberglass under the same test conditions. This can be proved further by the results shown in both Fig. 1 and Fig. 3: the 15% graphite PTFE has a much higher FCP speed than 15% fiberglass PTFE has, and, accordingly, it has a lower energy release rate, $J^*$, than 15% fiberglass PTFE has.

### 4.4. Fatigue crack propagation parameters

The values of $da/dN$, $J^*$, and $\dot{W}_i$ with respect to crack length were established from FCP experiments for each material. If the experimental results are in accordance with the MCL model, Equation 14, a plot of $(J^*/a)$

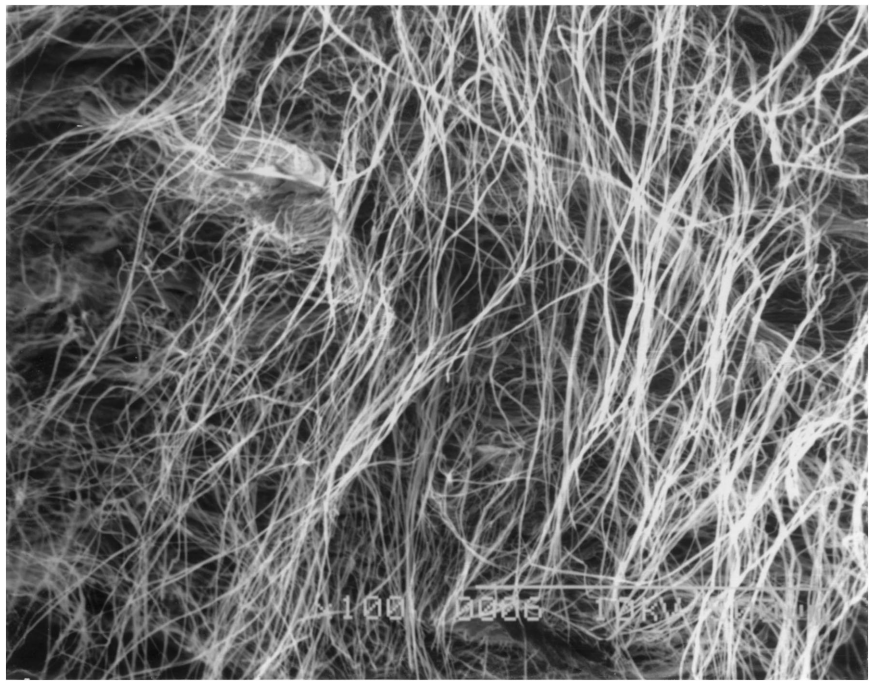

(a)

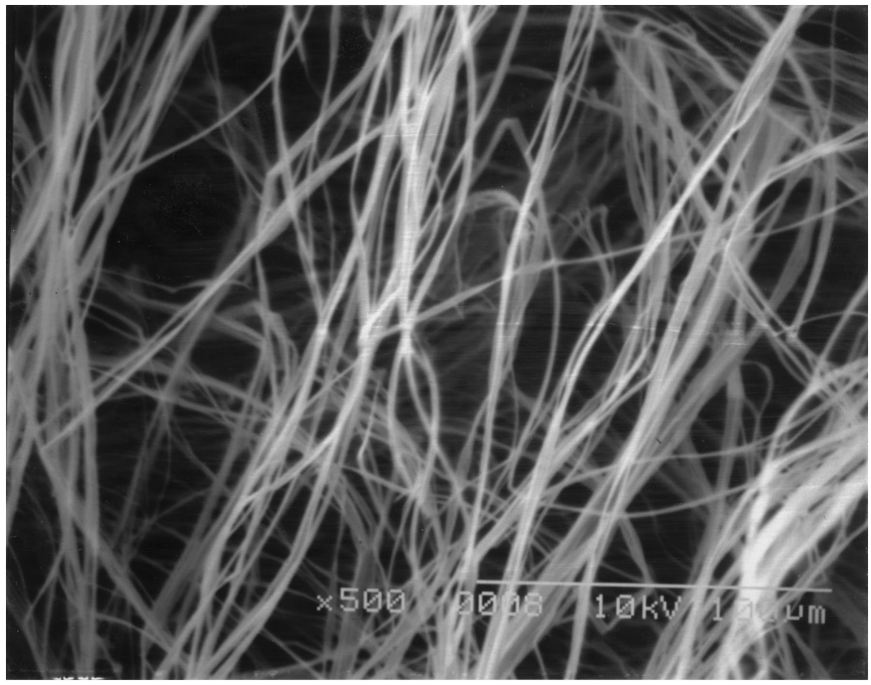

(b)

*Figure 7* Micrograph of damage species on the fracture surface within the stage of stable crack propagation for the virgin PTFE (a) 100×, (b) 500×.

versus $\dot{W}_i/[a(da/dN)]$ should give a straight line. Indeed, this is the case, as shown in Fig. 5a, b, and c, respectively. Straight lines are obtained for the four PTFE materials, where $\gamma'$ is the intercept and $\beta'$ is the slope of the lines. This attests to the applicability of the MCL model to describe the FCP in virgin PTFE, 15% fiberglass PTFE, 15% graphite PTFE, and 25% fiberglass PTFE. The values of $\gamma'$, being a material property-related parameter for evaluating FCP of these four kinds of PTFE materials, are listed in Table I.

It can be seen in Table I that $\gamma'$ decreases from 4700 kJ/m$^3$ for the virgin PTFE to 1150 kJ/m$^3$ for the 25% fiberglass PTFE. A higher value of $\gamma'$ indicates higher resistance to FCP since more energy is required to cause a unit volume of the material to change from an undamaged state to a damaged state. This analysis is basically in agreement with the test results of crack

TABLE I FCP parameter $\gamma'$ for the four PTFE materials

| Type of materials | Parameter $\gamma'$ (kJ/m$^3$) |
|---|---|
| Virgin PTFE | 4700 |
| 15% fiberglass PTFE | 2000 |
| 15% graphite particle PTFE | 1640 |
| 25% fiberglass PTFE | 1150 |

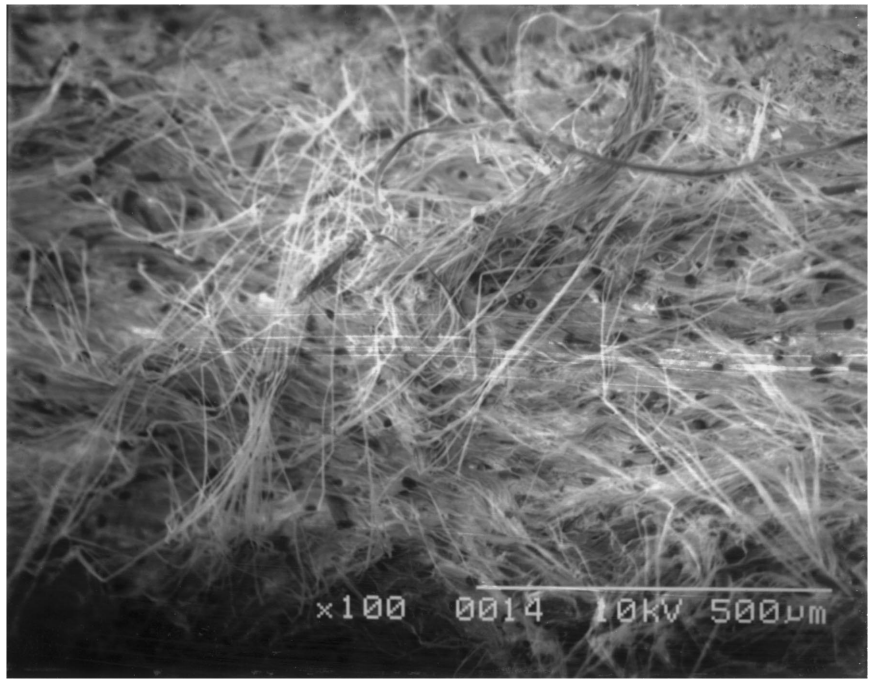


(a)

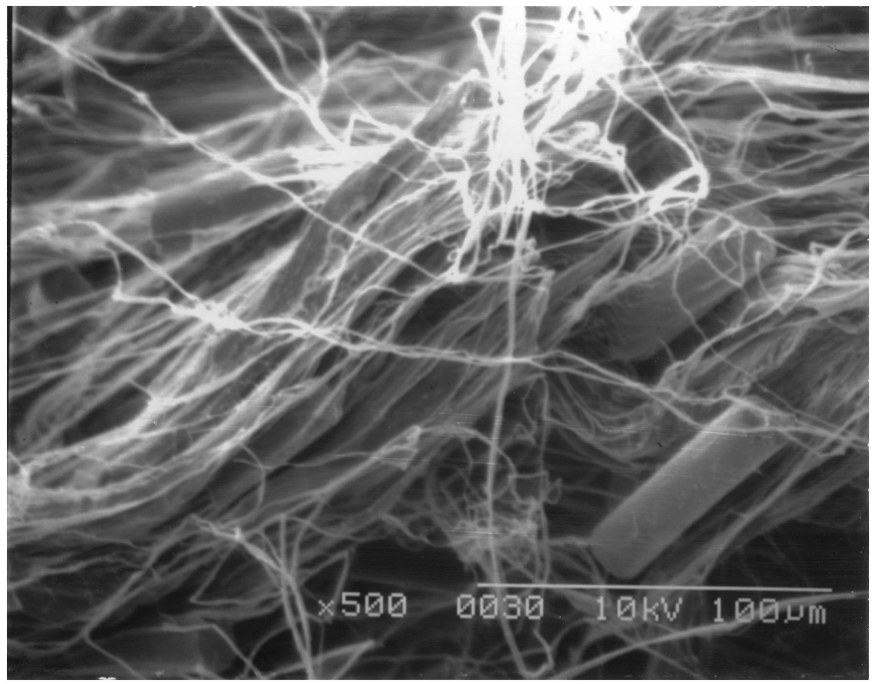


(b)

*Figure 8* Micrograph of damage species on the fracture surface within the stage of stable crack propagation for the 15% fiberglass-filled PTFE (a) 100×, (b) 500×.

length ($a$) versus fatigue cycles ($N$) and the energy release rate versus crack length, as shown in Figs 1 and 3. Virgin PTFE has the greatest value of $\gamma'$, thus showing the greatest resistance to FCP. For 15% fiberglass PTFE, its $\gamma'$ value ranks the second; thus, it also shows a considerably great resistance to FCP. Then comes the 15% graphite particle PTFE composite. For the same filler, the higher the content, the less the $\gamma'$ and hence a lower resistance to FCP.

The FCP speed versus the energy release rate for the four PTFE materials based on the experimental data is shown in Fig. 6. It can be seen from Fig. 6 that the overall tendency of $da/dN$ versus $J^*$ fits the $\gamma'$ criteria given in Table I. Although these four PTFE materials may belong to the same fluorocarbon family, the materials themselves are considerably different in nature, due to the different filler types and content, and processing conditions. In all of the tested materials, the MCL model closely describes FCP behavior over the entire range of the crack driving force. Again the curve displays the familiar S-shaped behavior, indicating three stages of FCP. A threshold stage is followed by a stage of reduced acceleration and then a stage of unstable crack propagation. This is indicative of crack tip damage associated with FCP, which has previously been investigated by Aglan and Moet [57].

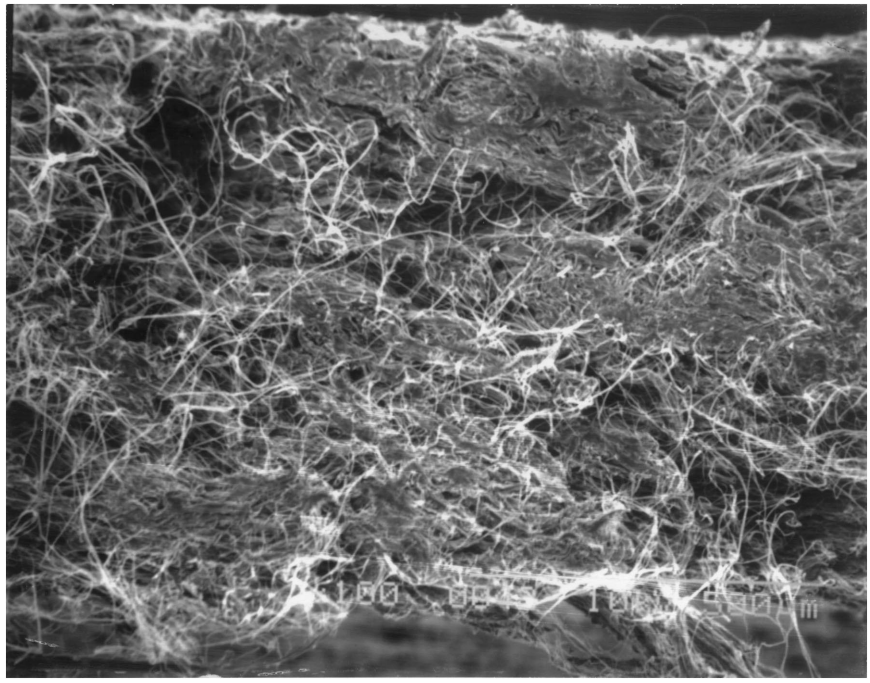

(a)

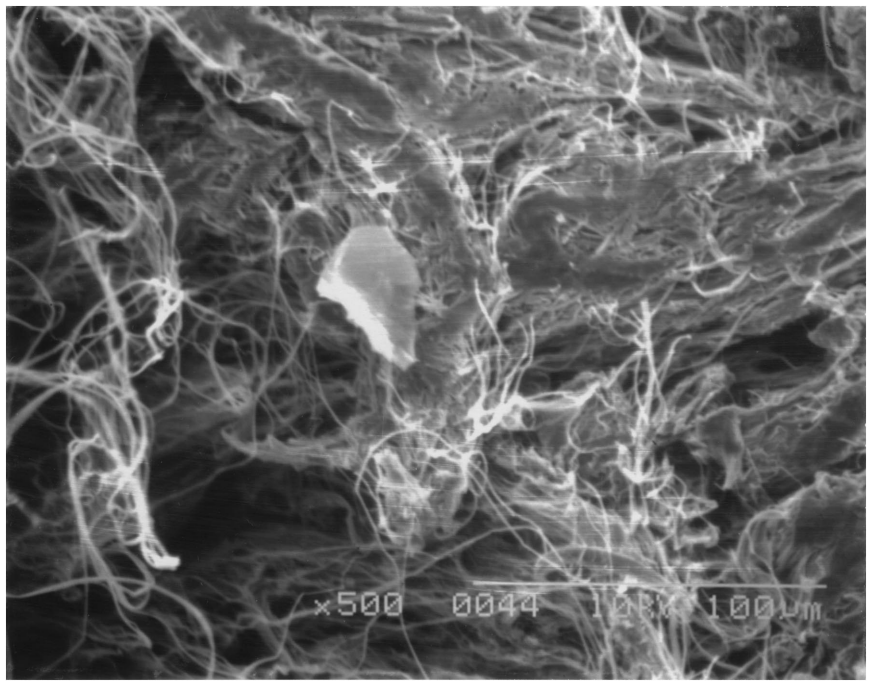


(b)

*Figure 9* Micrograph of damage species on the fracture surface within the stage of stable crack propagation for the 15% graphite particle-filled PTFE (a) 100×, (b) 500×.

### 4.5. $\gamma'$-Fatigue damage relationships

It is of great technical interest to relate the fatigue global behavior or macrobehavior represented here by $\gamma'$ of these materials to their microbehavior as determined by microstructure analysis of their damage species associated with FCP. The micrographs in Figs 7–10 are taken from an area on the fracture surface corresponding to the second stage of crack propagation in each material where damage is the responsible factor for crack retardation.

The micrographs shown in Fig. 7 are for the virgin PTFE at 100× and 500×. At low magnification (Fig. 7a), the ductile tearing feature of the PTFE is clearly shown. Microfibrils and drawn ligaments are the major damage species. At higher magnification (500×) in Fig. 7b, the fracture surface is covered by strong interlaced microfibrils. As can be seen from both figures, a large volume of PTFE material was involved in the fatigue damage process, indicating an extremely high energy dissipated in damage formation and evolution. This is manifested by the intensive fibrillation and ductile tearing of the matrix into severely drawn ligaments with very fine size. This is in accordance with the fatigue data analysis that the highest value of $\gamma'$

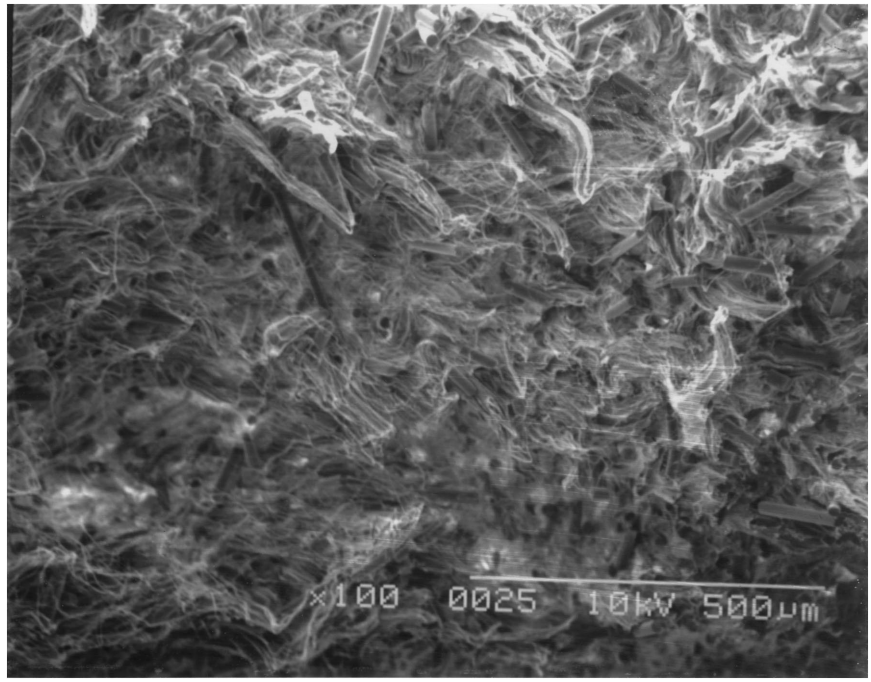


(a)

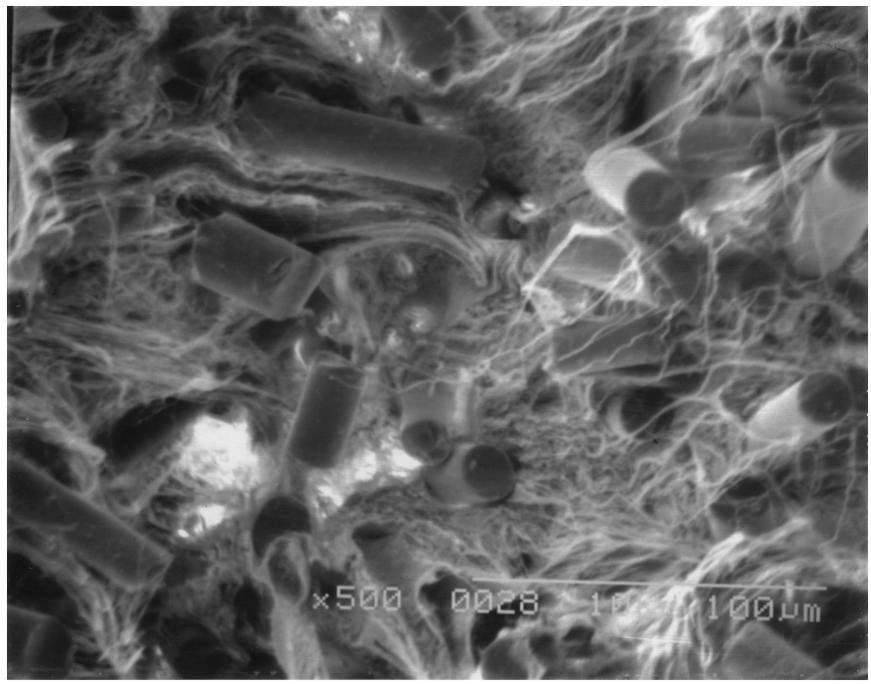


(b)

*Figure 10* Micrograph of damage species on the fracture surface within the stage of stable crack propagation for the 25% figberglass-filled PTFE (a) 100×, (b) 500×.

(4700 kJ/m$^3$) is obtained for the virgin PTFE among all the four PTFE materials considered in the present work, as shown in Table I.

The micrographs shown in Fig. 8 for the 15% fiberglass-filled PTFE, taken from the second region (stage of crack deceleration) similar to Fig. 7. At the magnification of 100× (Fig. 8a), it can be seen that the surface is covered with a considerable amount of ligament bundles and microfibrils. A few pulled-out glass fibers can be found in the lower right part of the graph in Fig. 8b. This indicates some fiber debonding from the PTFE matrix during fatigue cracking. The fracture surface features are more pronounced at higher magnification of 500× (Fig. 8b). Fibrillation, well-drawn ligament bundles, and grooves or microvoids can be clearly seen. In comparison with the virgin PTFE (Fig. 7b), less fibrillation is observed. In addition, the drawn ligaments underneath the fibrillation appear to be larger in size in comparison with the underlying structure in the virgin PTFE. Nevertheless, these drawn ligaments and the surface fibrils have dissipated a fairly large amount of energy as reflected in the specific energy of damage $\gamma'$ (2000 kJ/m$^3$).

The micrographs in Fig. 9 are for the 15% graphite particle-filled PTFE. At the magnification of 100× (Fig. 9a), very little fibrilation can be seen on the

fracture surface. Voids can be readily found on the fracture surface, as shown in the left side of the micrograph (Fig. 9a). The weak interfacial strength results in debonding of graphite particles from the matrix. At higher magnification (Fig. 9b), graphite particles can be seen in the matrix at different locations. Fibrillation similar to that of the 15% fiberglass-filled PTFE is observed. The drawn ligaments are not so pronounced with less ductile tearing, however. Overall, the fracture surface of the 15% graphite particle–filled PTFE appears to have a more brittle texture. The specific energy of damage for this material is 1640 kJ/m$^3$, which is about 80% of that of the 15% glass fiber–filled PTFE material.

Figure 10 presents the micrographs for the 25% fiberglass-filled PTFE taken from the typical area corresponding to the second stage of crack propagation. A large amount of glass fiber pulled-out, limited fibrillation, and microvoids can be seen from the low magnification (100×) micrograph (Fig. 10a). At higher magnification of 500×, the matrix shows a very limited amount of ductile tearing, and there exists quite a large amount of pulled-out glass fiber. Voids or grooves formed from the fiber pull-out are quite frequent. Fiber pull-out with clean surfaces indicates the weak nature of interfacial bonding between glass fiber and PTFE matrix. Much less fibrillation with very little tearing is evident in comparison with the 15% fiberglass-filled PTFE. Broad areas of matrix appear to pull up but do not continue to form microfibrils. Such fracture surface features indicate a low energy consumption process during FCP. This explains the lowest specific energy of damage $\gamma'$ (1150 kJ/m$^3$) for the 25% fiberglass-filled PTFE material.

## 5. Conclusions

FCP analysis was performed on four materials from the fluorocarbon family, namely virgin PTFE, 15% glass fiber PTFE, 15% graphite particle PTFE, and 25% glass fiber PTFE. The MCL model was employed to extract the specific energy of damage $\gamma'$, a material parameter characteristic of the FCP resistance of the materials. Based on the current investigation, the following conclusions can be drawn:

- Fillers (either short fibers or particulates) tend to decrease the fatigue fracture resistance of PTFEs.
- The fatigue fracture resistance also decreases with the increase in the filler dosages.
- Particulate filler tends to decrease the fatigue fracture resistance of PTFE, more than short fibrous filler at the same dosage does.
- The FCP kinetics of PTFE composites displays the familiar S-shaped character. Three stages of crack propagation were observed. The threshold stage is followed by a stage of reduced acceleration, where most damage is formed, approaching the stage of critical (unstable) crack propagation.
- There is a strong correlation between the fatigue fracture resistance, $\gamma'$, and the amount of damage associated with the stage of reduced acceleration, as determined by fracture surface analysis using scanning electron microscopy. Materials with a larger amount of damage exhibit a higher resistance to fatigue fracture.


## Acknowledgements

This work was sponsored by NASA Kennedy Space Center under contract number NAG10-0168.


## References


1. UNITED STATES INTERNATIONAL TRADE COMMISION, "In the matter of certain curable fluoroelastomer composition and precursors thereof" (International Trade Commission, Washington, D.C., 1995).
2. I. FRANTA, "Elastomers and rubber compounding materials, studies in polymer science," Vol. 1 (Elsevier Science Publishing Company Inc., New York, 1989) p. 294.
3. D. C. BLACKLEY, "Synthetic Rubbers: Their Chemistry and Technology" (Applied Science Publishers, London, 1983) pp. 283–287.
4. Wilden Pump and Engineering Co., 1997, U.S. Patent No. 5611678.
5. Albert Trostel Packings Ltd., 1997, U.S. Patent No. 5607168.
6. J. E. TURNER, "A summary of laboratory testing performed to characterize an elastomeric O-ring material to be used in the redesigned solid rocket motors of the space transportation system," NASA Technical Report, George C. Marshall Space Flight Center, Alabama, 1993.
7. J. H. PLUMBRIDGE, *J. Mater. Sci.* **7** (1972) 939.
8. J. A. MASON and R. W. HERTZBERG, *Crit. Rev. Macromol. Sci.* **1** (1973) 433.
9. Z. H. STACHURSKI, *Progress in Polymer Science* **22** (1997) 407–474.
10. J. H. DILLON, *Adv. Colloid Sci.* **3** (1950) 219.
11. B. ROSEN, "Fracture Processes in Polymeric Solids" (Wiley Interscience, New York, 1964).
12. I. WORLOCK and S. NEWMAN, "Fracture Processes in Polymeric Solids" (Wiley Interscience, New York, 1964) p. 235.
13. R. F. LANDEL and R. F. FEDORS, *ibid.* p. 361.
14. E. H. ANDREWS, "Physical Basis of Yield and Fracture," Conf. Ser. No. 1 (Institute of Physics and Physical Society, Woodbury, 1966) p. 127.
15. *Idem*, "Fracture of Polymers" (American Elsevier, New York, 1968).
16. *Idem*, in "Testing of Polymers," Vol. 4, edited by W. Brown (Wiley Interscience, New York, 1969) p. 237.
17. C. B. BUCKNELL, K. V. GOTHAM and P. I. VINCENT, in "Polymer science, a materials handbook", edited by A. D. Jenkins (American Elsevier, New York, 1972).
18. P. I. VINCENT, *Encycl. Polym. Sci. Technol.* **7** (1968) p. 292.
19. J. W. S. HEARLE, *J. Mater. Sci.* **2** (1967) p. 474.
20. P. BEARDMORE and S. RABINOWITZ, in "Plastic Deformation of Materials," edited by R. J. Arsenault (Academic Press, New York, 1975) p. 267.
21. J. M. SCHULTZ, in "Properties of Solid Polymeric Materials," edited by R. J. Arsenault (Academic Press, New York, 1977) p. 599.
22. C. B. BUCKNELL, "Toughened Plastics" (Applied Science Publ., London, 1977).
23. *Idem, Adv. Polym. Sci.* **27** (1978) 121.
24. M. J. OWEN, in "Composite Materials," edited by L. J. Brautman, Vol. 5 (Academic Press, New York, 1974) Chaps. 7 and 8.
25. B. HARRIS, *Composites* **8** (1977) 214.
26. E. H. ANDREWS and P. E. REED, *Adv. Polym. Sci.* **27** (1978) 1.
27. J. G. WILLIAMS, *Adv. Polym. Sci.* **27** (1978) 67.
28. H. H. KAUSCH, in "Polymer Fracture," edited by H. H. Kausch, (Springer-Verlag, New York (1978) p. 5.
29. J. U. STARKE, G. SCHULZE and G. H. MICHLER, *Acta Polymerica* **48** (1997) 92–99.
30. V. TANRATTANAKUL, W. G. PERKINS, F. L. MASSEY, A. MOET, A. HILTNER and E. BAER, *J. Mater. Sci.* **32** (1997) 4749–4758.

31. Y. SHA, C. Y. HUI, A. RUINA and E. J. KRAMER, *Acta Meterialia* **32** (1997) 3555–3563.
32. H. R. BROWN, *Macromolecules* **24** (1991) 2752.
33. M. IBNABDELJALIL and W. A. CURTIN, *Acta Meterialia* **45** (1997) 3641–3653.
34. H. J. SUE, J. D. EARLS and R. E. HEFNER, JR., *J. Mater. Sci.* **32** (1997) 4031–4037.
35. ASTM Standard, "Standard test methods for plane strain fracture toughness," E399-81, 1981.
36. H. AGLAN, *Carbon* **31** (1993) 1121–1129.
37. A. AHOGON and A. N. GENT, *J. Polym. Sci. Polym. Phys. Ed.* **13** (1975) 1903.
38. H. GREENSMITH, *J. Appl. Polym. Sci.* **7** (1963) 933.
39. R. ELLEITHY, H. AGLAN and A. LETTON, 1996. *J. Elastomers Plastics* **28** (1996) 199–222.
40. C. WANG and C. CHANG, *J. Polym. Sci. B, Polym. Phys.* **35** (1997) 2003–2015.
41. *Idem*, *ibid*. 2017–2027.
42. P. R. HORNSBY and K. PREMPHET, *J. Mater. Sci.* **32** (1997) 4767–4775.
43. A. SHAN, E. V. STEPANOV, A. HILTNER, E. BAER and M. KLEIN, *Int. J. Fracture* **84** (1997) 159–173.
44. H. AGLAN, "Fracture Morphology of Selective Polymer Systems Under Monotonic and Fatigue Loading," NASA Technical Annual Report (NASA John F. Kennedy Space Center, Florida, 1996).
45. P. C. HARRIS and F. J. ERDOGAN, *J. Basic Eng. Trans.* **85D** (1963) 528.
46. H. AGLAN, I. SHEHATA, L. FIGUEROA and A. OTHMAN, "Structure-Fracture Toughness Relationships of Asphalt Concrete Mixtures," Transportation Research Board Paper No. 92011 (National Academy of Science, Washington, D.C., 1992).
47. E. SANCAKTAR, *J. Adhesive Sci. Technol.* **9** (1995) 119–147.
48. G. SNOPPY, N. R. NEELAKANTAN, K. T. VARUGHESE and S. THOMAS, *J. Polym. Sci. B, Polym. Phys.* **35** (1997) 2309–2327.
49. H. AGLAN, *Int. J. Damage Mechanics* **2** (1993) 53–72.
50. *Idem*, *J. Elastomers Plastics* **25** (1993) 307–321.
51. H. AGLAN, A. OTHMAN, L. FIGUEROA and R. ROLLINGS, in "Transportation Research Board 1417" (TRB, Washington, D.C., 1993) pp. 178–186.
52. H. AGLAN, A. OTHMAN and L. FIGUEROA, in "Transportation Research Board 14149" (TRB Washington, D.C., 1994) pp. 57–63.
53. *Idem*, *J. Mater. Sci.* **29** (1994) 4786–4792.
54. H. AGLAN and Z. ABDO, *J. Adhesion Sci. Technol.* **10** (1996) pp. 183–198.
55. Z. ABDO and H. AGLAN, *ibid* **11** (1997) 941–956.
56. R. B. SEYMOUR, "Engineering Polymer Sourcebook" (McGraw-Hill Publishing Company, New York, 1990) pp. 213–222.
57. H. AGLAN and A. MOET, 1989. *Int. J. Fract.*, **40** (1989) 285.

*Received 16 December 1997*
*and accepted 15 January 1998*